Available online at www.sciencedirect.com
ScienceDirect
Journal of Sound and Vibration 324 (2009) 622–639
JOURNAL OF SOUND AND VIBRATION
www.elsevier.com/locate/jsvi

Frequency loci veering due to deformation in rotating tyres

I. Lopez*, R.R.J.J. van Doorn, R. van der Steen, N.B. Roozen, H. Nijmeijer

Section Dynamics and Control, Department of Mechanical Engineering, Eindhoven University of Technology, P.O. Box 513, 5600 MB Eindhoven, The Netherlands

Received 28 May 2008; received in revised form 18 February 2009; accepted 24 February 2009
Handling Editor: C.L. Morfey
Available online 31 March 2009

Abstract

This paper shows that the eigenfrequencies of a deformed tyre exhibit a mutual repulsion behaviour if the rotation velocity is increased. This phenomenon is known as frequency loci veering and is induced by the a-periodicity resulting from the tyre deformation due to the weight of the car. The corresponding eigenmodes interact in the transition zones and finally interchange. This is not the case for the undeformed tyre, where it is well known that rotation splits the eigenfrequencies around the eigenfrequencies of the non-rotating tyre. The change in eigenfrequencies is linearly related to the rotation velocity and is determined by the circumferential wavenumber and tyre radius only. For the undeformed tyre no modal interaction occurs as a consequence of rotation. Furthermore, modal interaction increases as tyre load increases and decreases as material damping increases. In previous work a methodology to model tyre vibrations has been developed, exploiting a modal base determined in a standard FE package and including rotational effects by a coordinate transformation. Major advantages of this approach are that the complex build-up of a tyre is retained and that the large (nonlinear) deformations and small (linear) vibrations are treated separately. In the present paper, the effects of deformation on the eigenfrequencies of a rotation tyre are examined using this methodology.

1. Introduction

The effects of rotation on the dynamic behaviour of a tyre are important in modelling the tyre/road noise caused by vibrational mechanisms. It is generally acknowledged that the main effect of rotation for the usual velocity range in tyres is a change of the wave velocities observed by an external observer (Eulerian reference frame) depending on the travelling direction [1–4]. In the Eulerian reference frame the speed of waves travelling in the direction of rotation increases while for waves propagating in the opposite direction the wave speed decreases by the same amount, which depends on the rotational velocity, wavenumber and tyre radius. This phenomenon is often referred to as Doppler effect.

Most of the published work on rotating tyres is based on the analysis of undeformed (unloaded) tyres. In Ref. [1] an equation is found which describes the symmetric split of the eigenfrequencies of an undeformed tyre when the rotational velocity increases. This equation can be used to map the non-rotating natural frequencies

*Corresponding author. Tel.: +31 40 247 2611; fax: +31 40 246 1418.
E-mail address: l.lopez@tue.nl (I. Lopez).

0022-460X/$ - see front matter © 2009 Elsevier Ltd. All rights reserved.
doi:10.1016/j.jsv.2009.02.038

on the natural frequencies of the rotating tyre in the wavenumber-frequency domain. Similarly, in Ref. [2] the vibration field of a rotating tyre is determined in a Lagrangian reference frame and the vibration field in the Eulerian reference frame is found by applying a Doppler shift in the wavenumber domain. Another possibility is to directly modify the speed of travelling waves according to the Doppler shift like in Ref. [3]. An alternative, FE-based, approach is presented in Ref. [4], where the motion of a rolling tyre is directly described in a Eulerian reference frame. Here the Doppler shift is also reported for the undeformed tyre. For the case of a loaded tyre, it is found that the eigenfrequency distribution decreases (modal density increases) as the rotational velocity increases.

From the above it can be concluded that the effect of rotation on the dynamic behaviour of unloaded tyres is known. It is unclear, however, what the effects of rotation on the dynamic response of a tyre are if the initial deformation of the tyre structure is included in the analysis. The purpose of this paper is to study the effects of rotation on the eigenfrequencies of a deformed (loaded) tyre. This is investigated by applying the approach presented in Ref. [5] to a realistic tyre model. It is shown that for a deformed tyre the eigenfrequencies do not cross when the rotational velocity increases, but show a mutual repulsion behaviour known as frequency loci veering. In addition, the real parts of the eigenvalues cross at the rotational velocity where the corresponding imaginary parts veer. Furthermore it is found that modal interaction increases as tyre load increases and decreases as material damping increases.

This paper is organised as follows. In Section 2 the approach to model vibrations on deformed rotating tyres from Ref. [5] is briefly reviewed and in Section 3.1 the used FE tyre model is described. Hereafter, Section 4 discusses the effects of rotation on the eigenfrequencies of a tyre, using the methodology described in Section 2, both for the unloaded and for the loaded situation. After that, the influence of the amount of loading and the presence and amount of damping is discussed in Section 5. Finally, the conclusions are summarised in Section 6.

2. Modelling approach

A methodology to model tyre vibrations up to 500 Hz on deformed rotating tyres is developed in Ref. [5]. Initially, the tyre is inflated and the initial tyre deformation is calculated using the full nonlinear system of equations. Subsequently, the modal base is constructed around the deformed state to include the effect of deformation on the eigenmodes of the tyre. After that, the mass matrix, eigenvalues and eigenvectors are extracted from the FE code and a coordinate transformation is applied to model rotation. As a consequence the stiffening of the tyre due to the centrifugal forces and the Coriolis effect are included in the model. A short review of the methodology to model rotation is given here.

In Ref. [5], the dynamic equations of a tyre in a Eulerian reference frame are obtained:

$$\ddot{\boldsymbol{\eta}}(t) + \tilde{\mathbf{D}}(\Omega)\dot{\boldsymbol{\eta}}(t) + \tilde{\mathbf{K}}(\Omega)\boldsymbol{\eta}(t) = \boldsymbol{\Phi}^T\mathbf{f}(t) \tag{1}$$

where $\boldsymbol{\eta}(t)$ are the modal coordinates of the tyre in the tyre reference frame, $\boldsymbol{\Phi}$ is the matrix of eigenvectors, $\mathbf{f}(t)$ is a column with forces acting on the tyre and

$$\tilde{\mathbf{D}} = 2\mathbf{P}(\Omega, \mathbf{M}, \boldsymbol{\Phi}) + \mathbf{D}_{\text{mod}} \tag{2}$$

$$\tilde{\mathbf{K}} = \mathbf{S}(\Omega, \mathbf{M}, \boldsymbol{\Phi}) + \mathbf{D}_{\text{mod}}\mathbf{P}(\Omega, \mathbf{M}, \boldsymbol{\Phi}) + \mathbf{K}_{\text{mod}} \tag{3}$$

The matrices $\mathbf{P}$ and $\mathbf{S}$ are added stiffness and damping terms due to the rotation

$$\mathbf{P}(\Omega, \mathbf{M}, \boldsymbol{\Phi}) = \boldsymbol{\Phi}^T\mathbf{M}\left(\hat{\boldsymbol{\Omega}}\boldsymbol{\Phi} + \Omega\frac{\Delta\boldsymbol{\Phi}}{\Delta\beta}\right) \tag{4}$$

$$\mathbf{S}(\Omega, \mathbf{M}, \boldsymbol{\Phi}) = \boldsymbol{\Phi}^T\mathbf{M}\left(\hat{\boldsymbol{\Omega}}^2\boldsymbol{\Phi} + 2\Omega\hat{\boldsymbol{\Omega}}\frac{\Delta\boldsymbol{\Phi}}{\Delta\beta} + \Omega^2\frac{\Delta^2\boldsymbol{\Phi}}{\Delta\beta^2}\right) \tag{5}$$

where $\hat{\boldsymbol{\Omega}}$ is a matrix relating the time derivative of the rotation matrix to the rotation matrix [5]. $\mathbf{K}_{\text{mod}}$ is a diagonal matrix with elements $k_{ii} = \omega_i^2$, where ω_i are the natural frequencies of the system, and if Rayleigh damping is considered, $\mathbf{D}_{\text{mod}}$ is a diagonal matrix with elements $d_{ii} = 2\xi_i\omega_i$, where ξ_i are the modal damping

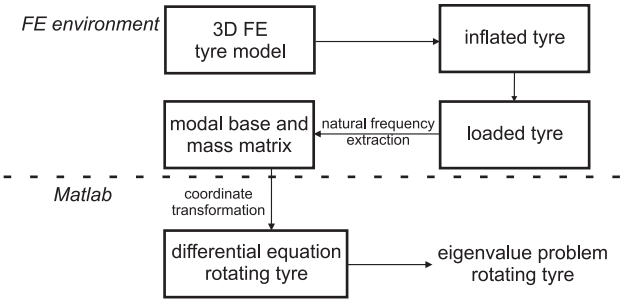

Fig. 1. Illustration of the approach to model vibrations on deformed rotating tyres.

ratios. The data needed to build the matrices $\tilde{\mathbf{D}}$ and $\tilde{\mathbf{K}}$ are the eigenvalues and eigenvectors of the tyre in the tyre reference system obtained from a FE model and $\mathbf{M}$ the mass matrix of the FE model. In addition, Ω stands for the rotational velocity of the tyre and β represents the spatial angle in the fixed reference frame. It should be noted that $\tilde{\mathbf{D}}$ and $\tilde{\mathbf{K}}$ are non-diagonal and non-symmetric matrices, which means that Eq. (1) is a coupled system of equations. Therefore the set of coordinates $\boldsymbol{\eta}(t)$ is not a set of modal coordinates of the tyre in the fixed reference frame. A new eigenvalue problem can be formulated for Eq. (1) in order to determine the eigenfrequencies and eigenvectors of the tyre in the fixed reference frame.

The system defined by Eq. (1) is transformed from a second-order to a first-order system and therefore a new vector $\mathbf{y}$ is defined as

$$\mathbf{y}(t) = \begin{bmatrix} \boldsymbol{\eta}(t) \\ \dot{\boldsymbol{\eta}}(t) \end{bmatrix} \tag{6}$$

The first-order system becomes

$$\mathbf{A}\dot{\mathbf{y}}(t) + \mathbf{B}\mathbf{y}(t) = \mathbf{r}(t) \tag{7}$$

with for $\mathbf{A}$, $\mathbf{B}$ and $\mathbf{r}$(t)

$$\mathbf{A} = \begin{bmatrix} \tilde{\mathbf{D}} & \mathbf{I} \\ \mathbf{I} & \mathbf{0} \end{bmatrix}, \quad \mathbf{B} = \begin{bmatrix} \tilde{\mathbf{K}} & \mathbf{0} \\ \mathbf{0} & -\mathbf{I} \end{bmatrix} \quad \text{and} \quad \mathbf{r}(t) = \begin{bmatrix} \boldsymbol{\Phi}^T \mathbf{f}(t) \\ \mathbf{0} \end{bmatrix} \tag{8}$$

Because $\mathbf{A}$ and $\mathbf{B}$ are non-symmetric matrices, a left and right eigenvalue problem exist resulting in different eigenvectors. However, the left and right eigenvalues are equal and solving the right eigenvalue problem gives the eigenfrequencies of the rotating tyre in the fixed reference frame

$$[\lambda\mathbf{A} + \mathbf{B}]\Psi = 0 \tag{9}$$

This leads to $2n$ eigenvalues λ_p and corresponding eigenvectors Ψ_p with $p = 1, 2, \ldots, 2n$. Again, it is important to note the rotational velocity dependency of $\mathbf{A}$ and $\mathbf{B}$ in Eq. (9) via $\tilde{\mathbf{D}}$ and $\tilde{\mathbf{K}}$. The approach from Ref. [5] summarised above is illustrated in Fig. 1.

3. FE tyre model

3.1. Model description

A FE model of a 185/70 SR14 tyre without tread pattern is used in this research [6]. The tread and sidewall consist of rubber, while the belts and carcass consist of fibre-reinforced rubber composites. The rubber is modelled as incompressible and hyperelastic. The hyperelastic behaviour of the rubber is described by a strain energy potential of the Neo-Hookean form. In addition, the fibre-reinforcements are modelled as a linear elastic material. In circumferential direction, 72 general three-dimensional 6- and 8-node linear hybrid brick

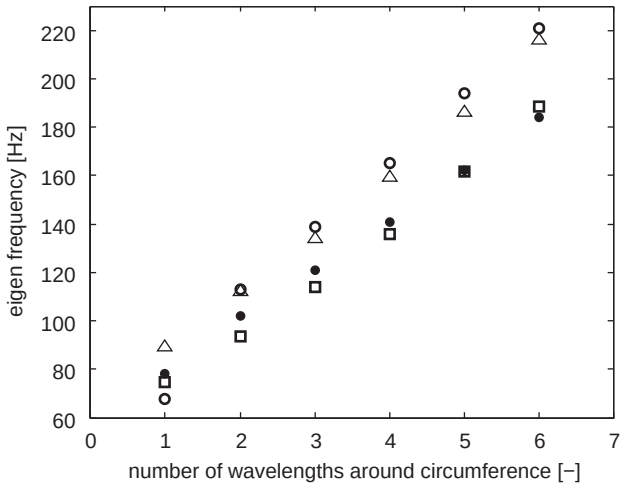

Fig. 2. Comparison of calculated and measured eigenfrequencies. • 185/70 R14 (calculated), △ 175/70 R13 [21], ○ 185/70 R14 [7], □ 195/70 R14 [22].

elements are used to discretise the model, each node having three active translational degrees of freedom (DOF). In total, this leads to a tyre model consisting of 6048 elements and to approximately 25,000 DOF. The tyre model is inflated to a uniform inflation pressure of 200 kPa. More detailed information about the build-up and materials of the FE model can be found in Ref. [6].

This FE tyre model has been qualitatively validated for the frequency range 0–250 Hz by comparing eigenfrequencies to experimental data of tyres of similar size, as shown in Fig. 2. Here the calculated eigenfrequencies of the first symmetric mode family $(n,0)$ (with n the number of wavelengths in the circumference) are compared to experimental data. However, the inner structure of the measured tyres is unknown, which prevents a direct comparison of the calculated eigenfrequencies with the measured results. Modal damping is assumed here with a fixed damping ratio $\xi_i = 0.04$ for all modes. This value has been estimated from the experimental modal analysis performed in Ref. [7] for frequencies up to 250 Hz and is in good agreement with damping values found in the literature (see e.g. Ref. [8]). The assumption of modal damping with a constant damping ratio for all modes is too simplistic for a tyre. However, this model allows for a qualitative analysis of the effect of rotation on the eigenfrequencies of a loaded tyre with the unloaded rotating tyre as reference, which is the goal of this paper.

3.2. Modelling tyre loading

The tyre is statically loaded onto an idealised rigid, flat and smooth surface. The normal to the surface is aligned with a radial direction in the tyre. The contact between the tyre and the smooth surface is modelled as a frictionless rigid contact. In order to simulate the static loading, the tyre rim is fixed and the surface is given a displacement in the normal direction (radial direction of the tyre). The magnitude of the displacement required to produce the desired reaction force at the tyre rim is obtained from the compression curve shown in Fig. 3. The displacements applied to obtain the results presented in this paper are summarised in Table 1.

The determination of the eigenmodes is a crucial step in a modal approach, since the tyre response is described via a superposition of the modeshapes. In the approach described in Section 2 the eigenvectors of a deformed (loaded) tyre are used to build the modal base. This allows to include the nonlinear effects due to the large deformations caused by the load. It is a well-known fact that an underformed tyre has multiple eigenvalues with multiplicity two and the corresponding modeshapes have equal forms but rotated by an amount $\pi/2n$. The absolute orientation of these two modeshapes is arbitrary. Deformation distorts the symmetry and for every multiple eigenvalue of the undeformed case there are two slightly different eigenvalues with corresponding modeshapes which have different forms [9]. Moreover, the orientation of the modes is no

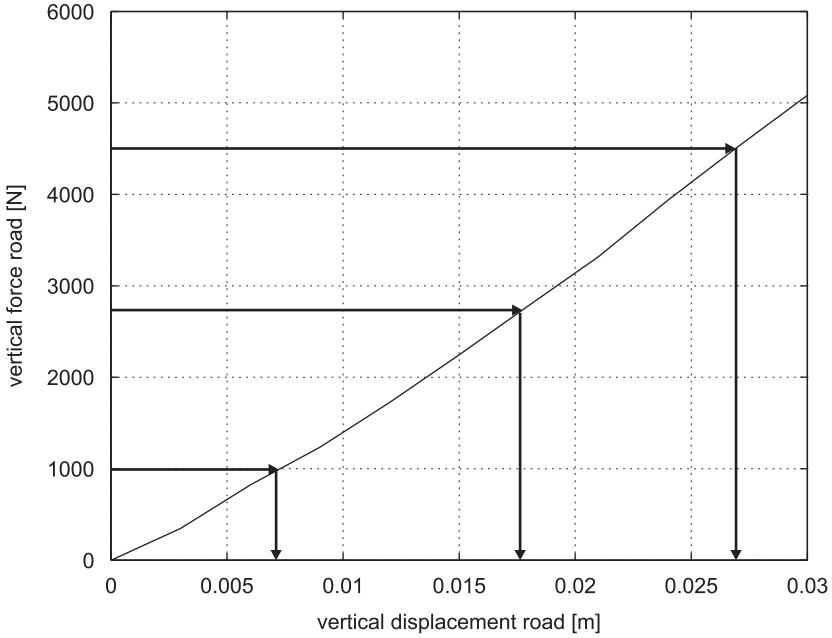

Fig. 3. Compression curve of the FE tyre model: vertical force versus vertical displacement.

Table 1
Tyre load and corresponding vertical displacement.

Tyre load (N)	Vertical displacement (mm)
1000	7.3
2750	17.8
4500	26.9

longer arbitrary due to the ground contact [9,10]. The naming convention introduced in Ref. [11] to distinguish between the two sets of eigenmodes of a deformed tyre is adopted here. The eigenmodes are classified in '0' and 'extremum' eigenmodes. The modeshapes corresponding to the '0' eigenmodes have zero radial displacement at the cross-section in the middle of the tyre–road contact area, while the modeshapes corresponding to the 'extremum' eigenmodes have a maximum radial displacement at that cross-section. Furthermore, eigenmodes will be named as (n,m) '0' or 'extr.' with $m = 0, 2, \ldots$ for the symmetric modes and $m = 1, 3, \ldots$ for the anti-symmetric modes.

Experiments show that applying a static load increases the eigenfrequencies compared to the eigenfrequencies of the undeformed tyre [10,11]. In Ref. [10], this frequency shift upwards is approximately 4% and 10% for the '0' and 'extremum' eigenmodes, respectively. In Fig. 4 the lowest 20 calculated eigenfrequencies for the unloaded and loaded tyre (load 2750 N) are shown. Generally, the eigenfrequencies of a tyre loaded by a force of 2750 N are approximately 2.5% ('0' modes) and 8.5% ('extremum' modes) higher compared with the undeformed situation. These percentages are in good agreement with the effect of tyre loading measured in Ref. [10].

3.3. Model reduction

The mass matrix of the FE tyre model is required to take rotational effects into account. However, exporting the mass matrix is not straightforward due to the dimensions of the mass matrix of a realistic tyre

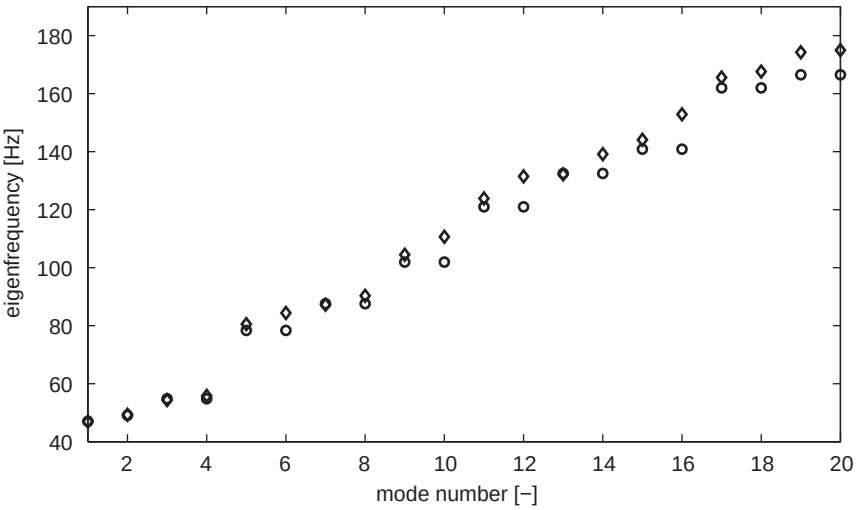

Fig. 4. Comparison of the eigenfrequencies of the unloaded (○) and loaded (◇) tyre for $F = 2750\,\mathrm{N}$.

model. Substructuring allows to reduce the number of DOF and computational costs. Reduction techniques split the DOFs into subsets (master and slave DOFs) and a transformation is applied to reduce the size of the system matrices, such that the response of the system is described in terms of the retained master DOFs only. Guyan reduction is adopted here, which neglects inertia effects and is exact at zero frequency only [12]. However, if the retained DOFs are selected following the guidelines reported in Ref. [13], a reduced eigenvalue problem can be obtained which gives a maximum error $<7\%$ between the full and the reduced models in the frequency range 0–500 Hz.

4. Effects of rotational velocity on the eigenfrequencies of a tyre

In this section, the methodology discussed in Section 2 is applied to the tyre model described in Section 3.1. The first 400 eigenmodes have been included in the calculations (frequency of the highest included eigenmode $\approx 600\,\mathrm{Hz}$). For the results in this section no damping has been included in the calculation ($\xi_i = 0$). The dynamic behaviour of an unloaded tyre is discussed first and these results are validated with the Doppler shift described in Ref. [1]. Hereafter, the effects of rotation on the eigenvalues of a loaded tyre are examined.

4.1. Rotating undeformed tyre

Fig. 5 shows the development of the eigenfrequencies of the undeformed non-rotating tyre up to 300 Hz versus rotational velocity. The solid lines are the eigenfrequencies obtained solving the eigenvalue problem (9). The crosses, which are plotted for increasing natural frequencies only, indicate the eigenfrequencies of the rotating tyre calculated by taking the Doppler shift at the eigenfrequencies of the non-rotating tyre into account. It can be seen that an excellent agreement exists between the eigenfrequencies found by solving the eigenvalue problem of a rotating tyre on one hand and the eigenfrequencies predicted by the Doppler shift on the other hand. The slight underestimation at the higher frequencies and higher rotational velocities is due to an error in the estimation of the spatial derivatives in Eqs. (4) and (5). These results have been calculated with a FE model with 72 elements in the circumference and a 7-point finite difference approximation of the derivatives. The discrepancy disappears if the number of elements and/or the order of the approximation are increased.

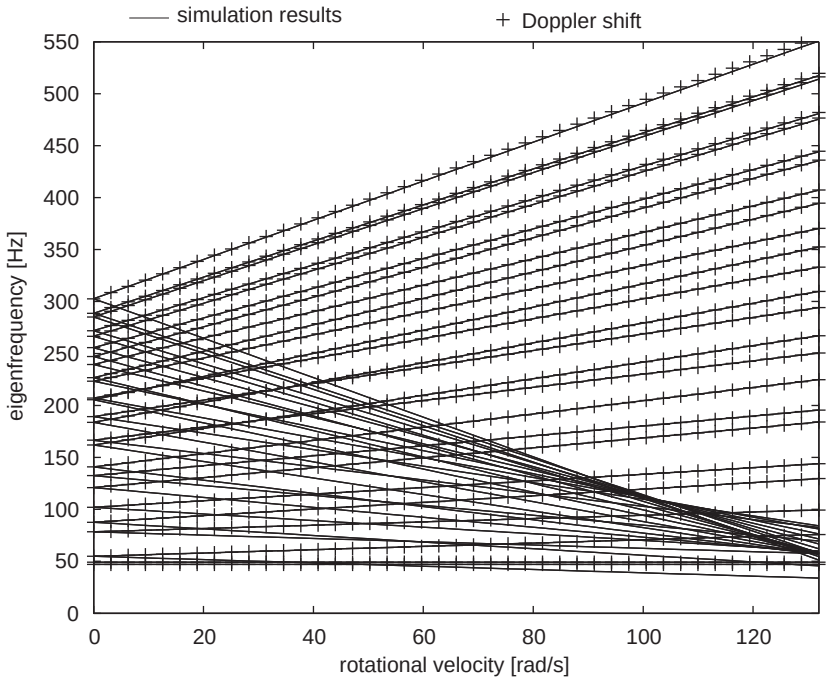

Fig. 5. Eigenfrequencies (Hz) versus rotational velocity (rad/s) of a rotating undeformed tyre (—) compared with the Doppler shift (++) applied to the eigenfrequencies of a non-rotating tyre.

4.2. Rotating deformed tyre

A flat smooth surface is pressed against the tyre with a force of 2750 N, which is derived assuming a total vehicle weight of approximately 1100 kg for a typical compact class car. Fig. 6 compares the eigenfrequencies of a deformed tyre (solid line) with the eigenfrequencies of an undeformed tyre (dashed line) in the frequency range 20–120 Hz.

An interesting phenomenon is visible here: eigenfrequency-lines approach each other and suddenly veer away instead of crossing. This results in high local curvature and the eigenfrequency-lines continue along the path that the other eigenfrequency-line would have taken if a crossing of the lines would have taken place. This phenomenon, referred to as 'frequency loci veering', 'avoided crossings', 'quasi-degeneracies' or 'mode crossovers' in the literature [14], has been noted in various structural systems (e.g. a curved beam, cables and chains, rotating circular string, coupled oscillators, multispan beams, coupled pendulums, blade assemblies and space structures) [15]. However, to the authors' knowledge, frequency loci veering has not been related to tyre dynamics so far.

Apparently some of the lines shown in Fig. 6 cross but if one looks more closely it becomes clear that, in the absence of damping, there are no line crossings at all (see Fig. 6(a)–(d)). This situation changes when damping is included, which will be discussed in detail in the next section.

The results shown in Fig. 6 also reveal that interaction occurs between eigenmodes of different families. So mode (2,1)'0' interacts with modes (1,0)'extr.' and (1,0)'0' (Fig. 6(a) and (b), respectively). To help the reader interpret Fig. 6 the eigenmodes corresponding to the first 14 eigenfrequencies are summarised in Table 2.

A close examination of Table 2 and Fig. 6 reveals that for the lower eigenmodes strong interaction (clear appearance of veering) only occurs between eigenmodes of the same family. However, this is not the case at higher frequencies, as can be clearly seen in Fig. 7, where the eigenfrequencies of the underformed (Fig. 7(a)) and the deformed (Fig. 7(b)) are plotted as a function of the rotational velocity in the frequency range 20–300 Hz up to a rotational velocity of 100 rad/s. The net effect of veering at higher frequencies (160–300 Hz) is that the eigenfrequency lines are curved instead of straight and the slope of these lines increases as the

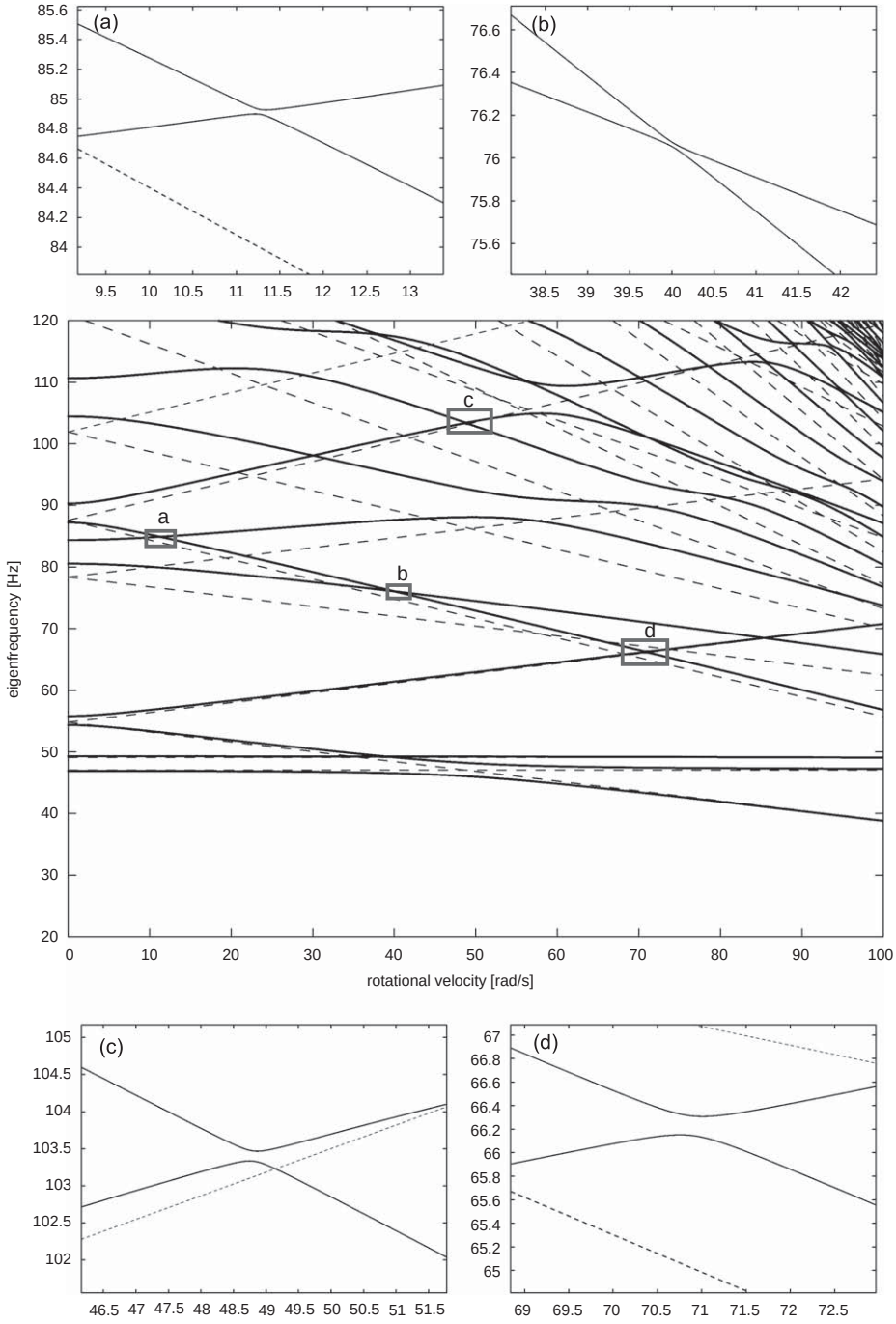

Fig. 6. Eigenfrequencies (Hz) versus rotational velocity (rad/s) of a rotating deformed tyre. $F = 2750$ N, 400 modes and no damping.

rotational velocity increases. An additional consequence of rotation is an increase of modal density. It can be seen in Fig. 7 that, as the rotational velocity increases, the number of modes below 300 Hz increases for both the unloaded and the loaded tyre.

Besides the effect of veering on the eigenfrequencies, the eigenmodes corresponding to two veering eigenfrequency lines interact also in the so-called transition zones and will finally interchange. More precisely,

Table 2
Lowest 14 eigenfrequencies and corresponding eigenmodes.

Eigenmode	Eigenfrequency (Hz)
(0,1)	46.9
torsion	49.3
(1,1)'extr.'	54.6
(1,1)'0'	55.8
(1,0)'0'	80.5
(1,0)'extr.'	84.4
(2,1)'0'	87.2
(2,1)'extr.'	90.3
(2,0)'0'	104.5
(2,0)'extr.'	110.6
(3,0)'0'	123.7
(3,0)'extr.'	131.5
(3,1)'0'	132.2
(3,1)'extr.'	139.2

Load 2750 N.

the involved modeshapes become coupled in the veering region and when the modes are spatially global, localisation occurs in this region and vice versa [16], a process often referred to as modal hybridisation in the literature. Generally, one might argue that modal hybridisation only affects the dynamic response if veering takes place over a broad velocity range [17]. However, Fig. 7 shows that for high velocities many eigenmodes are permanently interacting with one or more other eigenmodes. In other words, the high modal density of a tyre structure leads to persistent mutual interaction between eigenmodes if the velocity is increased. This interaction occurs between all modes, therefore also between symmetric and anti-symmetric modes, which means that they cannot be studied separately.

5. Frequency loci veering in rotating deformed tyres

5.1. Influence of the amount of loading

It has been shown in the literature, e.g. [14], that veering occurs in discrete as well as in continuous systems. The discretisation of a structure can even be the cause of the occurrence of veering, as is demonstrated in Ref. [18] for a square plate with identical boundary conditions all around. However, it is also shown that veering can be an inherent behaviour of asymmetric, a-periodic or disordered vibrating structures [18,14]. The occurrence of veering in rotating deformed tyres is not attributed to the discretisation of the tyre, but it is attributed to the deformation of the tyre, causing a small a-periodicity in a system with multiple eigenvalues which gives rise to frequency loci veering. The loading of the tyre causes the eigenfrequencies of the tyre to become simple (algebraic multiplicity = 1) and sufficiently close for frequency loci veering to occur. In Fig. 8 a schematic view of the deformed tyre geometry for the unloaded and loaded situation for three different loads is given. The plot corresponds to the circumference that passes through the middle of the tyre cross-section, which is symmetric in this case.

It can be seen that for a load of 1000 N the periodic symmetry of the tyre is only slightly distorted whereas for the nominal load of 2750 N and the higher load of 4500 N a clear flattening of the tyre can be seen. In Fig. 9 the eigenfrequencies of the deformed tyre as a function of rotational velocity are shown for the frequency range 20–160 Hz. Three different load values and no damping have been used.

At a first glance the three figures seem very similar but a closer look reveals that veering becomes more apparent as the load increases. This can be seen by, for example, looking at the lines in the velocity interval 55–65 rad/s and frequency range 100–110 Hz. In this region modes (2,1)'extr.' and (3,1)'0' interact and the interaction becomes stronger as tyre loading is increased; the distance between the frequency lines becomes larger and veering occurs over a broader velocity interval. At rotational velocities above the veering region the

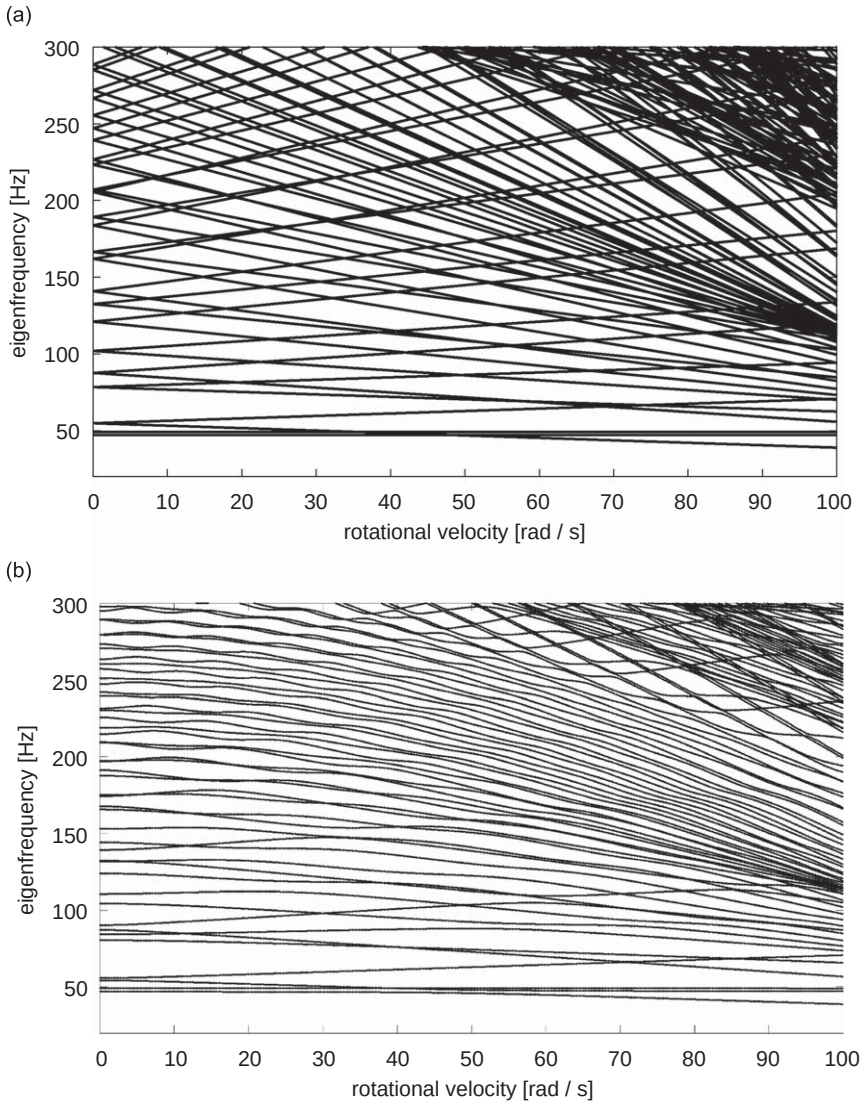

Fig. 7. Eigenfrequencies (Hz) versus rotational velocity (rad/s) in the frequency range 20–300 Hz; 400 modes and no damping. (a) Unloaded and (b) loaded 2750 N.

eigenmodes are interchanged, i.e. the upper branch corresponds to mode (2,1)'extr.' and the lower branch to mode (3,1)'0'. In the veering region or transition zone the eigenmodes are a combination of these two and can no longer be classified as a 2- and 3-nodal diameter mode. As mentioned earlier this effect is known as mode localisation or modal hybridisation. A similar behaviour can be observed at rotational velocities and frequencies of 50 rad/s and 50 Hz and 30 rad/s and 150 Hz.

In Fig. 10 the effect of tyre loading at higher frequencies can be seen, where the eigenfrequencies as a function of rotational velocity are shown for three different load values in the frequency range 160–300 Hz. In this frequency range clear differences can be seen, especially between Fig. 10(a) and (b) (load of 1000 and 2750 N, respectively). For the lowest load case no significant effect of veering can be seen at the higher frequencies (above 200 Hz) up to rotational velocities of 70 rad/s nor at higher rotational velocities for the frequency lines corresponding to higher order modes with $m = 0, 1$. However, despite the apparent absence of veering it should be noted that, in the absence of damping, none of the lines shown in Fig. 10(a) cross, but veer away. For the higher tyre loading values it is clear that strong interaction occurs between all eigenmodes, which implies that symmetric ($m = 0$) and anti-symmetric ($m = 1$) modes cannot be considered separately,

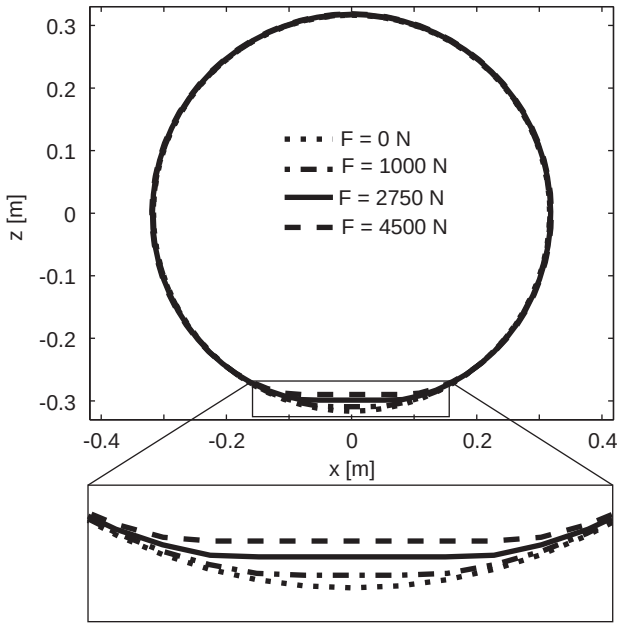

Fig. 8. Effect of tyre loading on tyre geometry.

since they interact with each other. Finally, the dense frequency lines at the upper-right corner of the figures correspond to eigenmodes of higher order families (2 or more nodal point in the cross-section), where the effect of veering is apparent for all three load values.

5.2. *Influence of damping*

In all results shown in this section, in order to keep the same axis scaling and facilitate the comparison of the plots for different damping values, the eigenvalues are normalised as follows:

- Normalised real part: $\mathrm{Re}(\lambda_i)/2\pi\xi_i$.
- Normalised imaginary part: $\mathrm{Im}(\lambda_i)/2\pi\sqrt{1-\xi_i^2}$.

Here the fact that, for proportional damping, the eigenvalues can be written as $\lambda_i = \xi_i\omega_i \pm j\omega_i\sqrt{1-\xi_i^2}$ has been used, where ω_i is the undamped eigenfrequency. Therefore at zero rotational velocity both the normalised real and the imaginary parts are equal (in absolute value) to the undamped eigenfrequencies ω_i of the non-rotating tyre independently of the value of ξ_i considered. It should be noted for non-zero values of the rotational velocities the normalised imaginary part can no longer be interpreted as the undamped frequency, since, due to rotation, the amount of damping changes and moreover the system is no longer proportionally damped.

It is suggested in Ref. [19] that strong mode localisation and veering of the eigenvalue loci are the two manifestations of the same phenomenon. Moreover, it is demonstrated in Ref. [19] that the eigenmodes corresponding to two veering eigenfrequency lines are interchanged after the so-called transition zones. Examining the behaviour of the real parts of the eigenvalues in a veering region can reveal this interchange of eigenmodes. It has been shown in Ref. [20] that the real parts of the involved eigenmodes cross in a veering region, which can be explained as an exchange of the damping of the involved modeshapes.

To illustrate the behaviour of the real part of the eigenvalues in a situation where no veering occurs the eigenfrequencies and corresponding normalised real parts for the underformed tyre are plotted in Fig. 11 as a function of rotational velocity for the nominal damping ratio $\xi_i = 0.04$. The real parts are negative which indicates that the tyre response is stable in this rotational velocity range. It is clear that for the undeformed

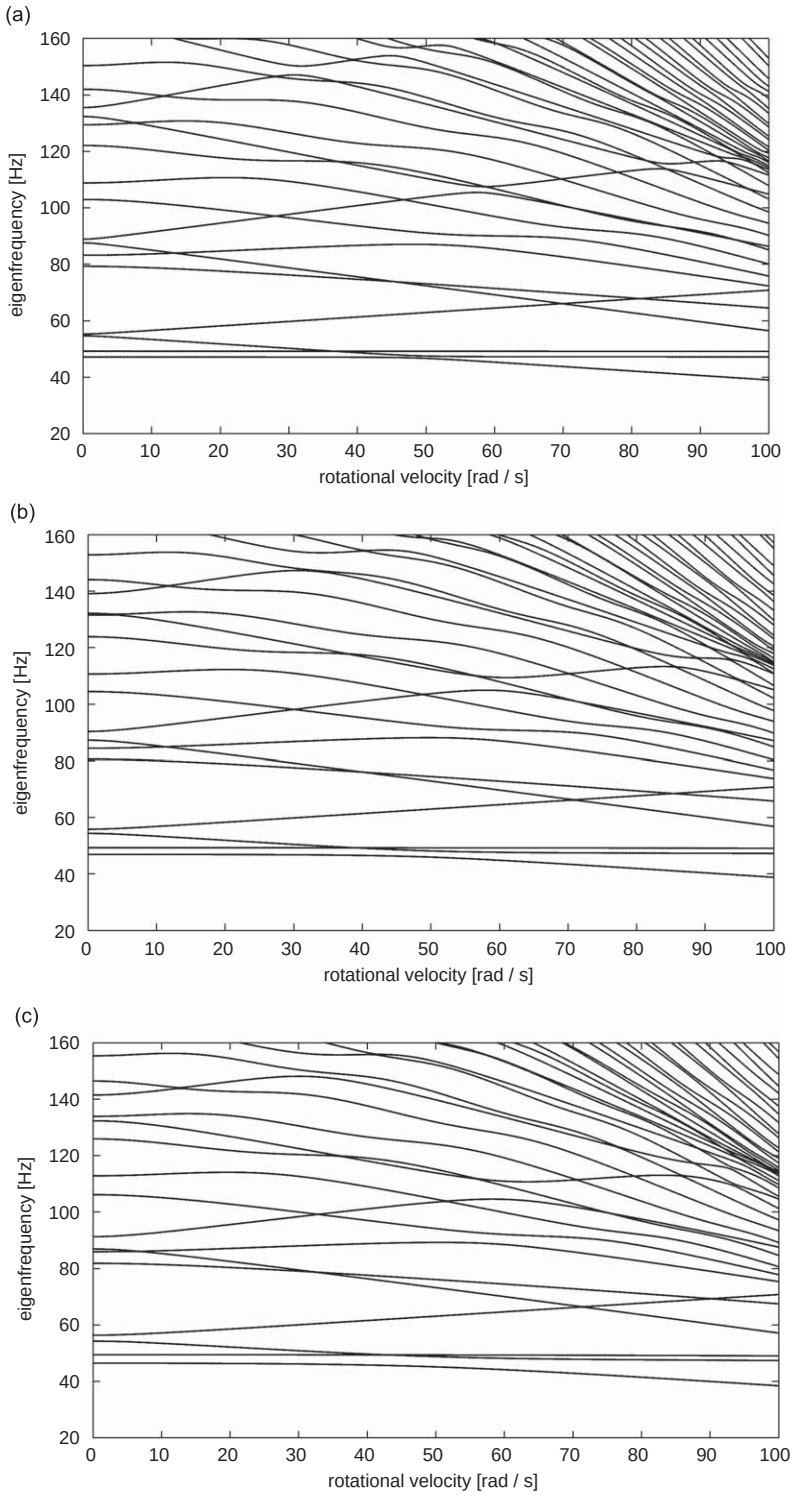

Fig. 9. Eigenfrequencies (Hz) versus rotational velocity (rad/s) in the frequency range 20–160 Hz; 400 modes and no damping. (a) 1000 N, (b) 2750 N, and (c) 4500 N.

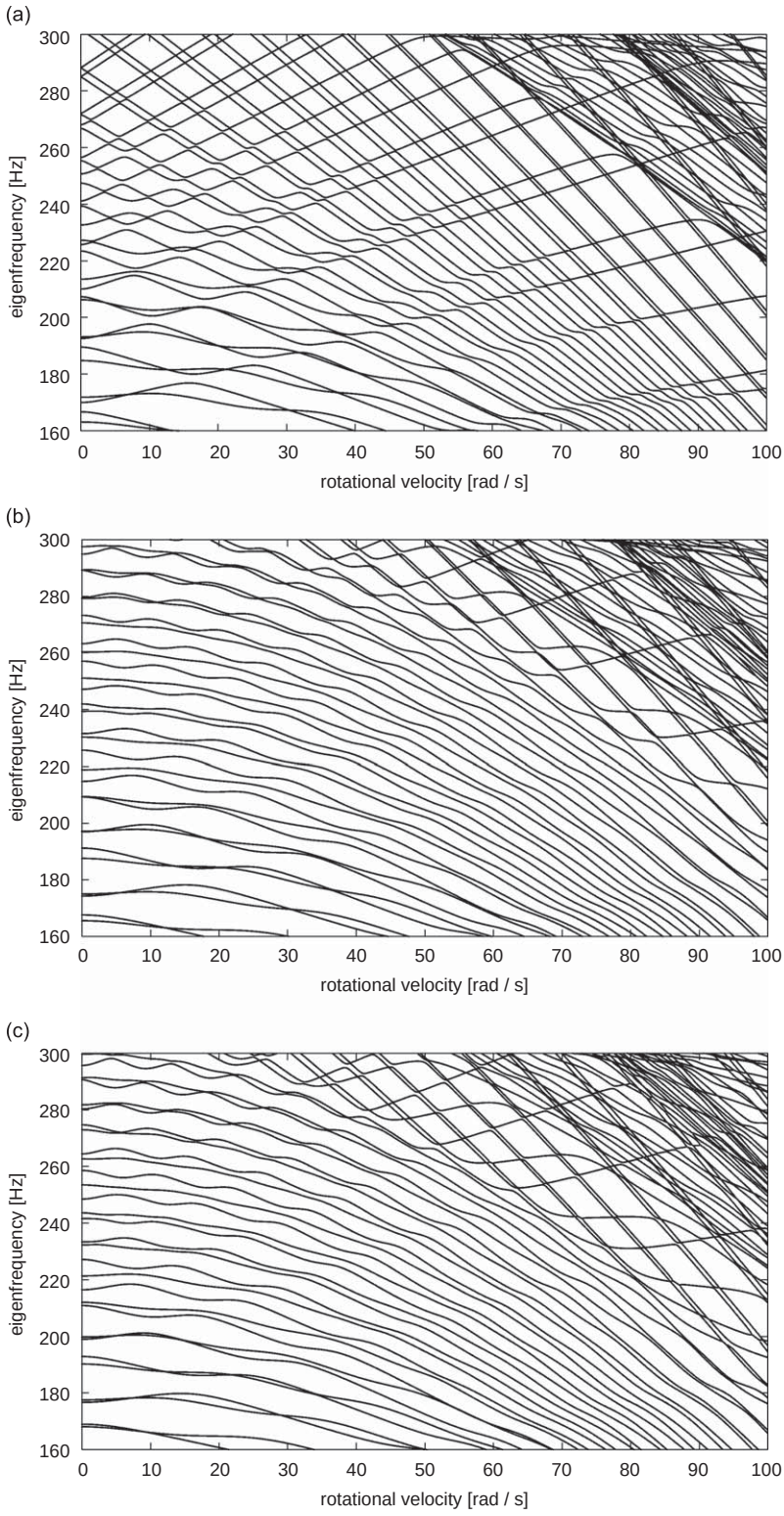

Fig. 10. Eigenfrequencies (Hz) versus rotational velocity (rad/s) in the frequency range 160–300 Hz; 400 modes and no damping. (a) 1000 N, (b) 2750 N, and (c) 4500 N.

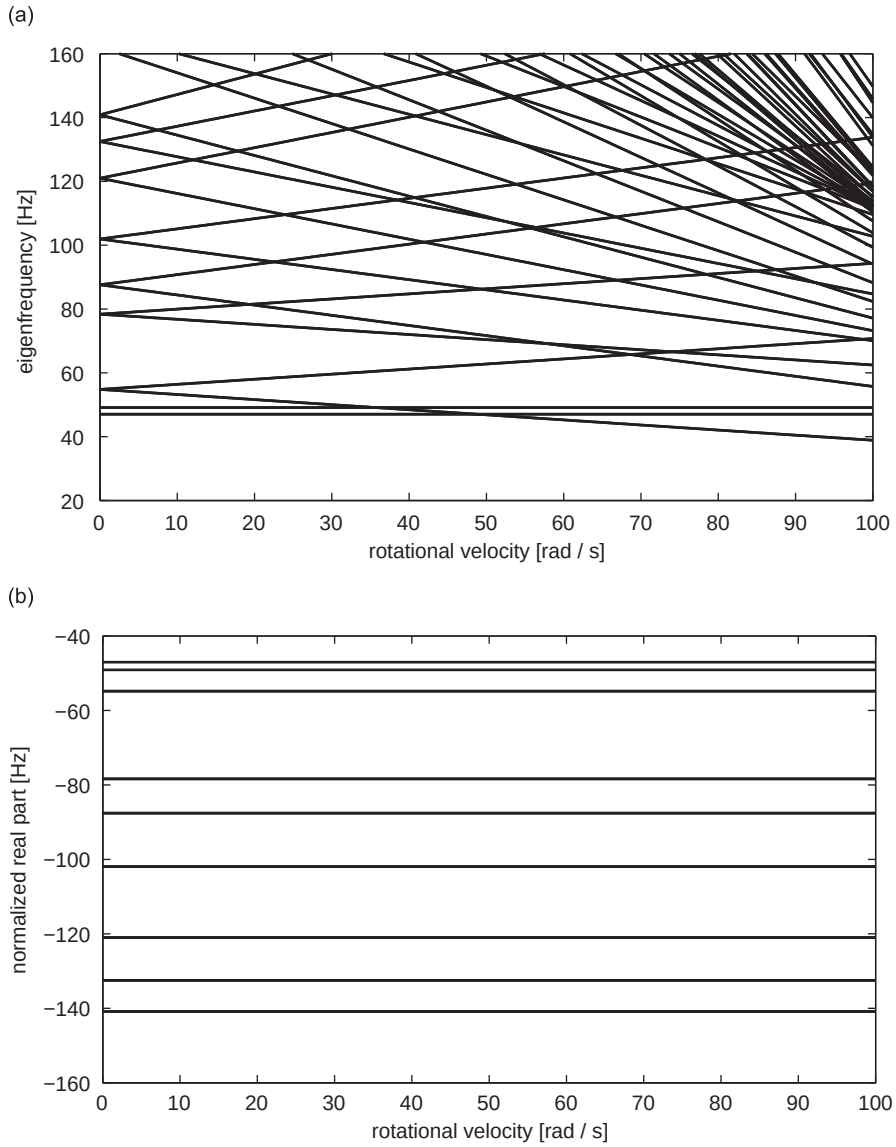

Fig. 11. Eigenfrequencies (Hz) (a) and normalised real part (Hz) (b) versus rotational velocity (rad/s). Undeformed tyre, 400 modes and $\xi = 0.4$.

tyre the real part of the eigenvalues remains constant as the rotational velocity increases and that the lines do not cross. This leads to the conclusion that the line crossings in the eigenfrequency plots are real crossings and no veering occurs.

In Figs. 12 and 13 the normalised imaginary and real part of the eigenvalues is shown as a function of rotational velocity for the deformed tyre for the nominal load of 2750 N and three different values of the damping ratio $\xi_i = 0.004, 0.04, 0.4$. In order to help the reader interpret the results, 12 regions where veering occurs for the undamped deformed tyre have been marked with rectangles and numbered as shown in Figs. 12(a) and 13(a). For example, rectangle 1 in Fig. 12(a) corresponds to rectangle 1 in Fig. 13(a). But in Figs. 12(b) and (c), and 13(b) and (c) only the regions where veering actually occurs have been marked. By looking at the evolution of the real parts as a function of the rotational velocity the occurrence of veering and modal interaction can be established. If the real parts of two eigenvalues cross, as is the case for rectangle 1

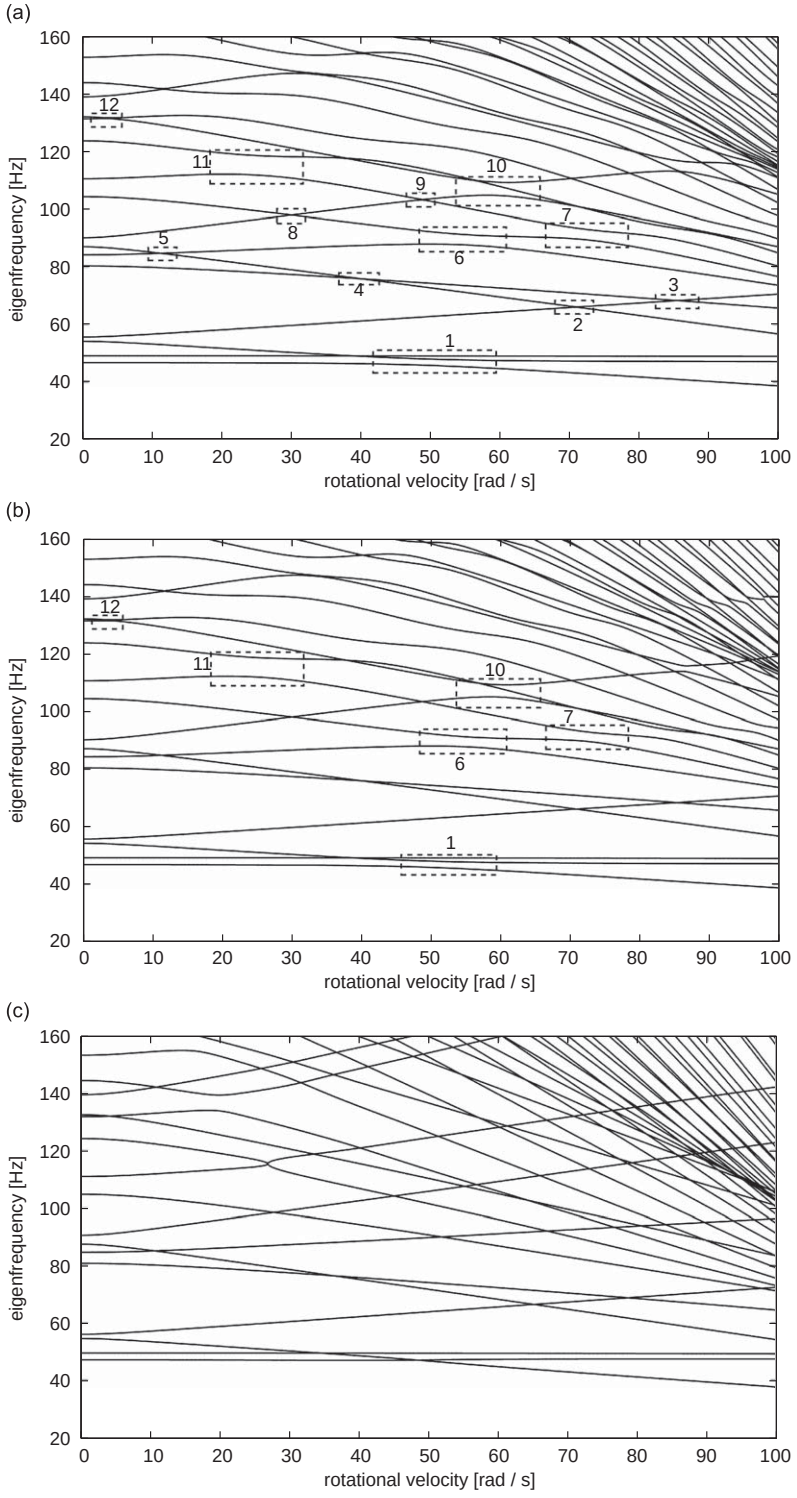

Fig. 12. Normalised imaginary part of the eigenvalues (Hz) as a function of rotational velocity (rad/s), load 2750 N and 400 modes. (a) $\xi = 0.004$, (b) $\xi = 0.04$, and (c) $\xi = 0.4$.

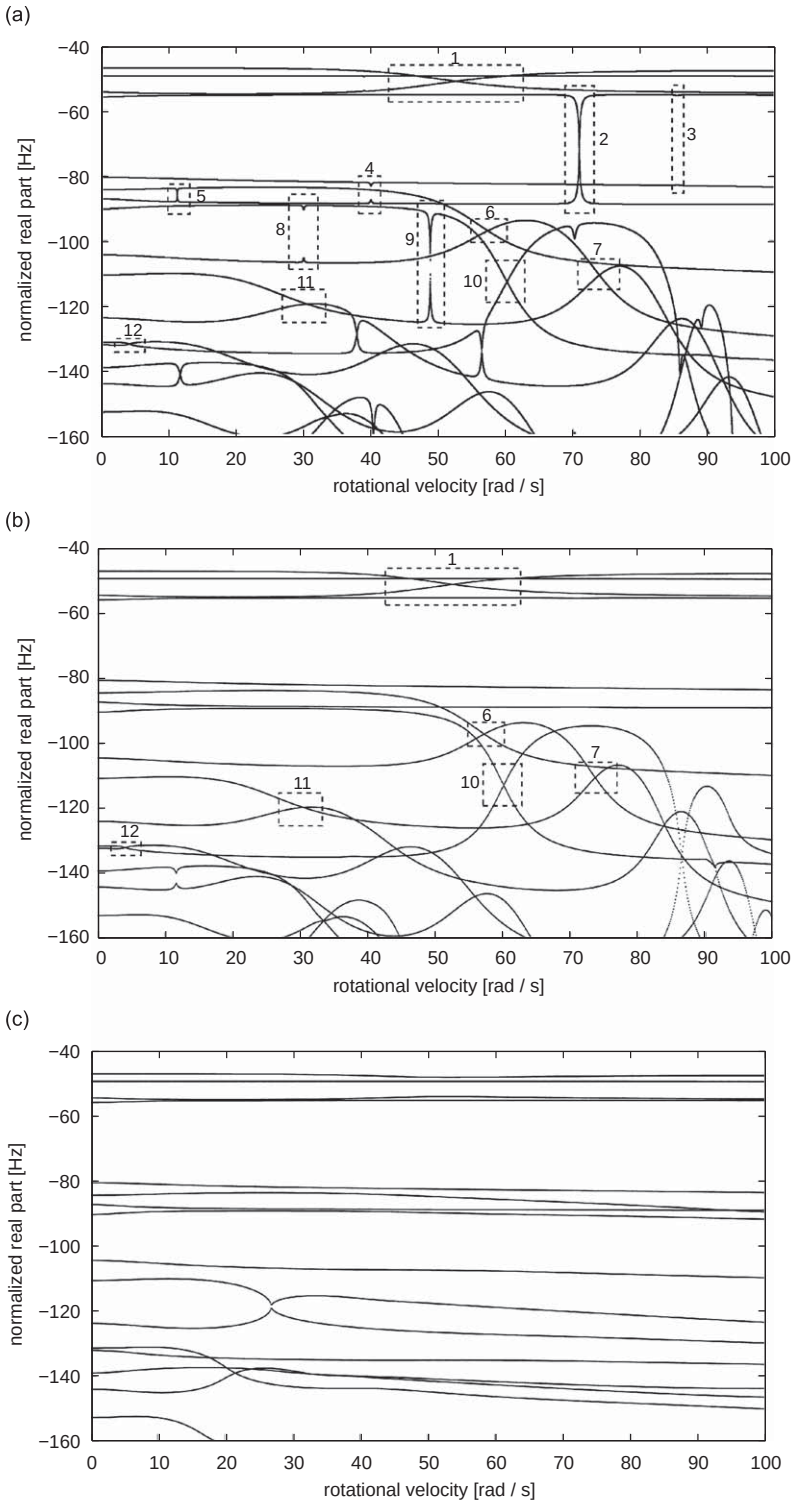

Fig. 13. Normalised real part of the eigenvalues (Hz) as a function of rotational velocity (rad/s), load 2750 N and 400 modes. (a) $\xi = 0.004$, (b) $\xi = 0.04$, and (c) $\xi = 0.4$.

Table 3
Influence of damping on the occurrence of veering.

Box	Lower mode	Higher mode	$\xi = 0$	$\xi = 0.004$	$\xi = 0.04$	$\xi = 0.4$
1	(0,1)	(1,1)'extr.'	Strong	Strong	Strong	None
2	(1,1)'0'	(2,1)'0'	Weak	Weak	None	None
3	(1,1)'0'	(1,0)'0'	Weak	None	None	None
4	(1,0)'0'	(2,1)'0'	Weak	None	None	None
5	(1,0)'extr.'	(2,1)'0'	Weak	Weak	None	None
6	(1,0)'extr.'	(2,0)'0'	Strong	Strong	Strong	None
7	(1,0)'extr.'	(3,0)'0'	Strong	Strong	Strong	None
8	(2,1)'extr.'	(2,0)'0'	Weak	None	None	None
9	(2,1)'extr.'	(3,0)'0'	Weak	Weak	None	None
10	(2,1)'extr.'	(3,1)'0'	Strong	Strong	Strong	None
11	(2,0)'extr.'	(3,0)'0'	Strong	Strong	Strong	None
12	(2,0)'extr.'	(3,1)'0'	Strong	Strong	Strong	None

Load 2750 N.

shown in Fig. 13(a), then it can be concluded that veering occurs and that the eigenmodes are interchanged in the transition region. This is in agreement with the behaviour of the real parts of the involved eigenvalues in a veering region shown in Ref. [20].

The plots shown in Figs. 12 and 13 have been carefully studied to determine whether veering occurs or not and the results are summarised in Table 3. The interaction is termed 'weak' if the crossing of the real parts occurs in a narrow rotational velocity interval and 'strong' if the real parts cross in a broader rotational velocity interval. The term 'none' means that the real parts do not cross and, therefore, no veering occurs.

It can be concluded from the results in Figs. 12 and 13 and Table 3 that damping has a significant influence on the occurrence of veering. Already very low values of the damping ratio cause some of the veering regions to disappear and if the damping increases to the experimentally determined nominal value ($\xi_i = 0.04$), only the veering regions where strong interaction occurs remain. If damping is further increased to unrealistically high values veering completely disappears and the eigenfrequencies tend to vary linearly with the rotational velocity as in the undeformed case. Although not plotted, the trend shown in Figs. 12 and 13 for the lower frequency range has also been found at higher frequencies.

6. Conclusions

In the present paper the effect of rotation velocity on the eigenvalues of a rotating deformed tyre has been studied. The presence of a phenomenon known as frequency loci veering has been revealed which is induced by the a-periodicity resulting from tyre loading. This a-periodicity leads to close eigenvalues with algebraic multiplicity 1. The effect of veering increases with both rotational velocity and frequency. Since a tyre is a modally rich structure for frequencies above 100 Hz, there is no space for eigenfrequencies to follow the path described by the Doppler shift. The 'neat' eigenvalue distribution for an undeformed rotating tyre predicted by the Doppler shift is not directly applicable to a deformed rotating tyre, since the evolution of the eigenvalues of a deformed tyre as a function of rotational velocity cannot be described by a linear relationship. Furthermore, veering is stronger as tyre load increases. Material damping has a significant influence on veering. When damping is included the number of eigenmodes that interact with each other decreases drastically (even for a small amount of damping) and the interaction becomes weaker. When damping is increased to unrealistically high values the eigenfrequencies tend to increase/decrease linearly with the rotational velocity. The implications of frequency loci veering for tyre/road noise predictions should be further investigated, but it is expected that veering will significantly affect the predicted dynamic response of the rotating tyre.

References

[1] Y.J. Kim, J. Bolton, Effects of rotation on the dynamics of a circular cylindrical shell with applications to tire vibration, *Journal of Sound and Vibration* 275 (2003) 605–621.

[2] F. Wullens, W. Kropp, Wave content of the vibration field of a rolling tyre, *Acta Acustica United with Acustica* 93 (2007) 48–56.

[3] R. Pinnington, A wave model of a circular tyre. Part 1: belt modelling, *Journal of Sound and Vibration* 290 (2006) 101–132.

[4] M. Brinkmeier, U. Nackenhorst, S. Petersen, O. von Estorff, A finite element approach for the simulation of tire rolling noise, *Journal of Sound and Vibration* 309 (2008) 20–39.

[5] I. Lopez, R. Blom, N. Roozen, H. Nijmeijer, Modelling vibrations on deformed rolling tyres—a modal approach, *Journal of Sound and Vibration* 307 (2007) 481–494.

[6] Simulia, *Abaqus Example Problems Manual*, sixth ed., 2006.

[7] J. Fioole, Experimental Modal Analysis of an Automobile Tire, Bachelor Project, Eindhoven University of Technology, 2008.

[8] M. Fraggstedt, Vibrations, Damping and Power Dissipation in Car Tyres, PhD Thesis, MWL, KTH, 2008.

[9] P.W.A. Zegelaar, Modal analysis of tire in-plane vibration, SAE Paper No. 971101.

[10] R. Pieters, Experimental Modal Analysis of an Automobile Tire Under Static Load, Bachelor Project, Eindhoven University of Technology, 2007.

[11] P. Kindt, F.D. Coninck, P. Sas, W. Desmet, Experimental modal analysis of radial tires and the influence of tire modes on vehicle structure borne noise, *31st FISITA 2006, World Automotive Congress*, 2006.

[12] R. Guyan, Reduction of stiffness and mass matrices, *AIAA Journal* 3 (1965) 380.

[13] N. Bouhaddi, R. Fillod, A method for selecting master dof in dynamic substructuring using the Guyan condensation method, *Computers and Structures* 45 (1992) 941–946.

[14] N. Perkins, C.D.M. Jr, Comments on curve veering in eigenvalue problems, *Journal of Sound and Vibration* 106 (1986) 451–463.

[15] X. Liu, Behavior of derivatives of eigenvalues and eigenvectors in curve veering and mode localization and their relation to close eigenvalues, *Journal of Sound and Vibration* 256 (2002) 551–564.

[16] S. Vidoli, F. Vestroni, Veering phenomena in systems with gyroscopic coupling, *Journal of Applied Mechanics* 72 (2005) 641–647.

[17] P. Marugabandhu, J. Griffin, A reduced-order model for evaluating the effect of rotational speed on the natural frequencies and mode shapes of blades, *Journal of engineering for gas turbines and power* 125 (2003) 772–776.

[18] B. Bhat, Curve veering: inherent behaviour of some vibrating systems, *Shock and Vibration* 7 (2000) 241–249.

[19] C. Pierre, Mode localization and eigenvalue loci veering phenomena in disordered structures, *Journal of Sound and Vibration* 126 (1988) 485–502.

[20] X. Chen, A. Kareem, Curve veering of eigenvalue loci of bridges with aeroelastic effects, *Journal of Engineering Mechanics* 129 (2003) 146–159.

[21] S. Gong, A study of In-Plane Dynamics of Tires, PhD Thesis, Delft University of Technology, 1993.

[22] B. Kim, G. Kim, T. Lee, The identification of sound generating mechanisms of tyres, *Applied Acoustics* 68 (2007) 114–133.